Letter

Tuning the nuclei-induced spin relaxation of localized electrons by the quantum Zeno and anti-Zeno effects

V. Nedelea,[1,2] N. V. Leppenen,[3] E. Evers,[1] D. S. Smirnov,[3,*] M. Bayer,[1] and A. Greilich[1,†]

[1]*Experimentelle Physik 2, Technische Universität Dortmund, 44221 Dortmund, Germany*

[2]*Istitute of Applied Physics, Moldova State University, MD2028, Moldova*

[3]*Ioffe Institute, 194021 St. Petersburg, Russia*

(Received 15 December 2022; accepted 25 July 2023; published 7 September 2023)

Quantum measurement back action is fundamentally unavoidable when manipulating electron spins. Here we demonstrate that this back action can be efficiently exploited to tune the spin relaxation of localized electrons induced by the hyperfine interaction. In optical pump-probe experiments, powerful probe pulses suppress the spin relaxation of electrons on Si donors in an InGaAs epilayer due to the quantum Zeno effect. By contrast, an increase of the probe power leads to a speed-up of the spin relaxation for electrons in InGaAs quantum dots due to the quantum anti-Zeno effect. The microscopic description shows that the transition between the two regimes occurs when the spin dephasing time is comparable to the probe pulse repetition period.

DOI: 10.1103/PhysRevResearch.5.L032032

Modification of quantum system dynamics due to the interaction with a measurement apparatus can always be described microscopically, for example, based on the Schrödinger equation [1,2]. In many cases, however, the general concepts of strong or weak measurements [3–6] can be applied. The former, also known as von Neumann type of measurements, is widely discussed nowadays for measurement-based quantum computation [7–9], while weak measurements are often implemented experimentally to minimize the system perturbation.

Frequent measurements can lead to freezing of the quantum dynamics, known as quantum Zeno effect [10,11], which requires measurements with a repetition period T_R shorter than the Zeno time [12], τ_Z, the time of non-Markovian relaxation. The less known and less universal is the quantum anti-Zeno effect which is the acceleration of the system relaxation due to the quantum back action [13–15]. It can occur when the repetition period is longer than the Zeno time [12]. In fact, this condition can be easily realized, but often the measurement involves additional heating and other perturbations, from which the quantum anti-Zeno effect can be challenging to separate.

The quantum Zeno effect is important for quantum information processing [16,17], especially with spin-based qubits, as it can be used to increase the electron spin relaxation time; the quantum anti-Zeno effect, by contrast, allows one to quickly erase spin polarization so that both effects should be taken into account when measuring spin qubits. However, the short Zeno time of free charge carriers strongly hinders reaching the regime of the quantum Zeno effect.

For localized electrons, the spin relaxation mechanisms [18] related to orbital electron motion, such as Elliot-Yafet [19,20], Bir-Aronov-Pikus [21], and Dyakonov-Perel [22], are suppressed. Then, the hyperfine interaction with the lattice nuclei plays the dominant role in electron spin relaxation [23,24]. Due to the long nuclear spin coherence times, the electron spin relaxation is hyperfine-induced and is essentially non-Markovian [25–27]. In this case, the Zeno time is of the order of the electron spin dephasing time T_2^* [28] making the quantum Zeno effects particularly important for localized electron spins [29–32]. As quantum dots represent attractive candidates for scalable quantum information processing, manifestations of the quantum Zeno effects were reported: suppression of tunneling [33–36], stabilization of optical emission [37–39], and nuclear spin freezing [40–42]. None of the previous studies, surprisingly, has addressed Zeno effects for the nuclei-induced spin relaxation of localized carriers experimentally.

In our work, we apply the optical pump-probe technique to manipulate the spin relaxation time of electrons localized in quantum dots or on donors, utilizing the quantum Zeno and anti-Zeno effects. Due to the scaling of the dephasing time with the localization volume, $T_2^* \propto \sqrt{V}$, we observe the opposite Zeno effects for these two systems for similar experimental conditions.

Experiment. The first sample consists of 20 layers of *n*-doped InGaAs self-assembled quantum dots (QDs) separated by 70 nm barriers of GaAs. A δ doping of Si 16 nm above each layer provides a single electron per QD on average. The QD density per layer is about $10^{10}\,\mathrm{cm}^{-2}$. Rapid thermal annealing at 880 °C for 30 s shifts the average emission energy to 1.3662 eV and reduces the spread of the QD size distribution [43]. The second sample consists of a 10 μm thick InGaAs epilayer with an indium fraction of 3%. It was grown

*smirnov@mail.ioffe.ru

†alex.greilich@tu-dortmund.de

Published by the American Physical Society under the terms of the Creative Commons Attribution 4.0 International license. Further distribution of this work must maintain attribution to the author(s) and the published article's title, journal citation, and DOI.

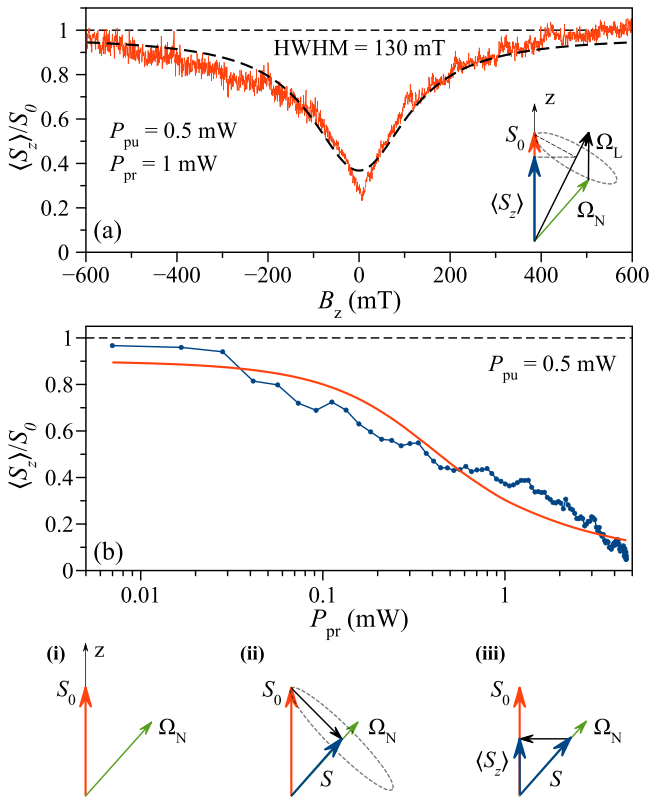

FIG. 1. (a) PRC (orange) for the QD sample with Lorentzian fit shown by the black dashed curve. The inset shows the mechanism of polarization recovery in Faraday geometry. (b) Probe power dependence of the zero field spin polarization $\langle S_z\rangle$ normalized by the S_0 measured at 1 T for the pump power $P_{pu} = 0.5$ mW (blue dots) with its theoretical fit (orange curve) with $P_\pi = 103$ mW, $T = 6$ K. The sketches below illustrate the microscopic origin of the anti-Zeno effect, see the theory part for an explanation.

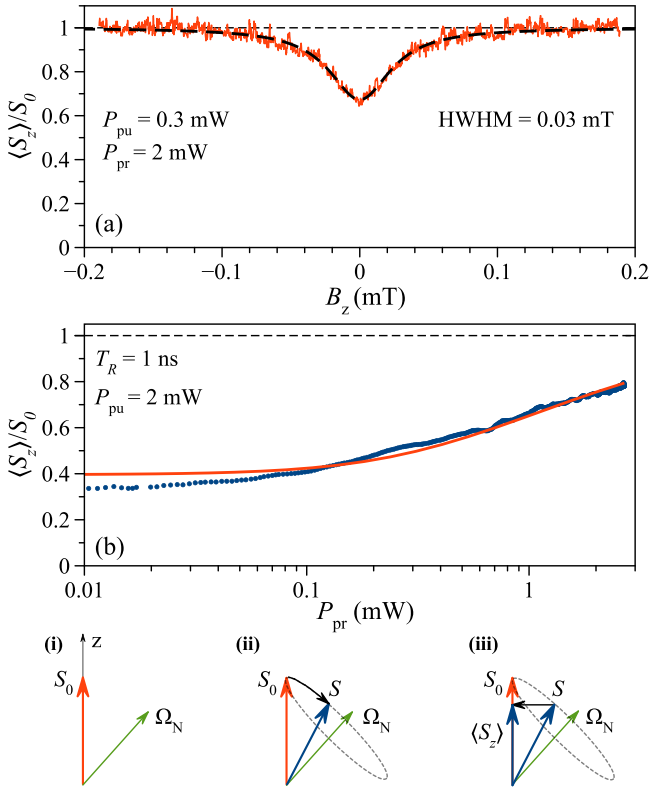

FIG. 2. (a) Exemplary PRC for the epilayer sample with the pump and probe powers stated by the labels. The black dashed curve gives the Lorentzian fit with the HWHM of 0.03 mT. (b) Probe power dependence of the normalized spin polarization (blue dots) with its theoretical fit (orange curve) with $P_\pi = 80$ mW. The sketches illustrate the microscopic mechanism of the quantum Zeno effect, see the theory part for an explanation.

by molecular beam epitaxy on a GaAs substrate. The sample was doped with Si atoms providing a donor carrier density of 3.9×10^{16} cm^{-3} [44].

We use the pump-probe technique to measure the spin dynamics using the Faraday rotation technique. We apply a longitudinal magnetic field parallel to the optical z axis (Faraday geometry). Localized spin-singlet trion complexes are resonantly excited for the QD sample and on the low-energy PL flank for the epilayer sample. The laser pulses with a duration of 2 ps are emitted with $1/T_R = 1$ GHz repetition frequency. Samples are cooled to a temperature of 6 K in a cryostat. The beams were focused on the sample into a spot with 50 μm diameter for the pump and 45 μm diameter for the probe, for which we measured the Faraday ellipticity. See Sec. S1.A of the Supplemental Material for further technical details and optical properties of samples.

Results. Figure 1(a) shows the spin polarization $\langle S_z\rangle$ of the QD sample as a function of the magnetic field for a -50 ps delay between pump and probe pulses, identical to a $+950$ ps delay, the pump power is $P_{pu} = 0.5$ mW and the probe power is $P_{pr} = 1$ mW. The trace is normalized to its value S_0 in high magnetic field of 1 T. At zero magnetic field, the spin polarization is reduced by the hyperfine interaction with the fluctuating nuclear spin bath of the host lattice [45]. The longitudinal magnetic field B_z decouples the electron spins from the nuclear environment and increases the spin polarization, leading to the polarization recovery curve (PRC) shown in Fig. 1(a). The inset in Fig. 1(a) shows a sketch of the spin stabilization: the projection of the average spin polarization $\langle S_z\rangle$ on the z axis rises to S_0 with increasing longitudinal magnetic field, shown by Ω_L, and Ω_N denotes the random Overhauser field.

The PRC can be approximately fit by a Lorentzian, see the black dashed line. The fit yields the half width at half maximum (HWHM) of 130 mT, which together with the electron longitudinal g factor $g_e = -0.69$ [43] gives the electron spin dephasing time $T_2^* = 0.13$ ns. It is smaller than the pulse repetition period $T_R = 1$ ns.

Then we scan the probe power and show the corresponding values of $\langle S_z\rangle/S_0$ in Fig. 1(b). This ratio decreases with increase of the pump power from one to zero, which reveals the decrease of the electron spin relaxation time in zero magnetic field. This corresponds to the quantum anti-Zeno effect.

In the epilayer sample, we observe the opposite behavior using the same method. Figure 2(a) shows a PRC example for $P_{pu} = 0.3$ mW and $P_{pr} = 2$ mW, together with a Lorentzian fit. The HWHM of the PRC, in this case, is only 0.03 mT, which is smaller than for the QD sample by more than three orders of magnitude, c.f. Fig. 1(a). This is related to the larger localization volume of electrons on shallow donors than in

QDs, the resulting weaker role of the hyperfine interaction, and, accordingly, the longer electron spin dephasing time T_2^* [44]. Further, Fig. 2(b) demonstrates the probe power dependence of the spin polarization $\langle S_z\rangle$ at zero magnetic field normalized to S_0 at the saturation value of 3 mT. In stark contrast to Fig. 1(b), the normalized spin polarization rises with increasing measurement strength, revealing the quantum Zeno effect.

The observation of opposite effects for the measurement impact in the two samples for the same probe pulse repetition period and similar other conditions calls for a theoretical foundation.

Theory. The spin dynamics of localized electrons between the pulses in the presence of hyperfine interaction with an external magnetic field applied is described by the Bloch equation [45]:

$$\frac{d\boldsymbol{S}}{dt} = (\boldsymbol{\Omega}_L + \boldsymbol{\Omega}_N) \times \boldsymbol{S} - \frac{\boldsymbol{S}}{\tau_s}. \tag{1}$$

Here $\boldsymbol{S}$ is the spin of the electron, $\boldsymbol{\Omega}_L = g_e \mu_B \boldsymbol{B}_z/\hbar$ is the Larmor frequency with μ_B being the Bohr magneton, $\boldsymbol{\Omega}_N$ is the spin precession frequency in the random Overhauser field of the nuclear spins, and τ_s is the additional phenomenological electron spin relaxation time related, for example, to the electron-phonon and spin-orbit interactions [46,47] [τ_s is typically independent of B, which agrees with the flat PRC in Figs. 1(a) and 2(a) in large magnetic fields]. The time scale of the nuclear spin dynamics is much longer than that of the electrons, so that $\boldsymbol{\Omega}_N$ can be assumed to be "frozen" [23] and described by the probability distribution function $\mathcal{F}(\boldsymbol{\Omega}_N) \propto \exp[-2(\Omega_N T_2^*)^2]$ [48]. Note that despite the pump helicity modulation, a small degree of nuclear spin polarization along the z axis can appear in the experiment [28], but it can be accounted for as an additional contribution to the external magnetic field.

The localized electron spins are pumped and probed optically through resonant spin-singlet trion excitation, with the probe pulses arriving in effect shortly before the pump pulses. Neglecting the electron spin dynamics between the probe and pump pulses [49], following the approach of Ref. [50] we find that the electron spin vectors before ($\boldsymbol{S}^-$) and after ($\boldsymbol{S}^+$), a pulse pair are related by

$$S_x^+ = q^2 Q S_x^-, \quad S_y^+ = q^2 Q S_y^-, \quad S_z^+ = S_z^- + g. \tag{2}$$

Here g is the spin polarization created by the pump pulse, $q = \cos(\pi/2\sqrt{P_{\rm pr}/P_\pi}) < 1$ describes the back action of the probe pulse [51] with P_π indicating the π pulse power [52]. The back action of the pump pulses is similarly described by Q [50] (the difference in the power of Q is related to the circular polarization instead of linear). In agreement with the general quantum mechanical postulates [53,54], the measurement of the z spin component destroys the transverse spin components S_x and S_y. Microscopically, this is related to the trion excitation, which obeys the selection rules for circular polarization [55] and erases the quantum coherence between the spin-up and spin-down electron states during the recombination [56]. In fact, $1 - q^2$ is the probability of trion excitation by the probe pulse [57]. We assume the pump and probe pulses to be exactly resonant with the optical transition, which maximizes the Faraday ellipticity signal and suppresses pulse-induced spin rotations [50].

The steady-state solution of Eqs. (1) and (2) yields the electron spin polarization S_z^- measured by the probe pulses [28]. This solution has to be averaged over the random nuclear fields to obtain the observed spin signal $\langle S_z\rangle$, while we neglect the distribution of all the other parameters for simplicity. Generally, this can be done only numerically [28], but in some limiting cases, we find transparent analytical expressions, which we give and discuss below.

A strong enough longitudinal magnetic field ($\Omega_L T_2^* \gg 1$) decouples the electron and nuclear spins. The spin relaxation, in this case, is Markovian with the time τ_s, so that the measurement back action is negligible. Assuming slow spin relaxation ($\tau_s \gg T_R$), we find that $\langle S_z\rangle$ equals to

$$S_0 = g\tau_s/T_R. \tag{3}$$

This gives spin polarization in the absence of hyperfine interaction.

At zero magnetic field, the electron-nuclei interaction leads to spin relaxation, and thus to a smaller average spin $\langle S_z\rangle$. This effect determines the amplitude and width of the PRC.

In the limit of $T_R \gg T_2^*$, relevant for the quantum anti-Zeno effect, pulsed excitation and detection can be described as continuous spin generation and relaxation due to the measurement back action:

$$\frac{d\boldsymbol{S}}{dt} = (\boldsymbol{\Omega}_N + \boldsymbol{\Omega}_L) \times \boldsymbol{S} - \frac{\boldsymbol{S}}{\tau_s} - \frac{1-q^2}{T_R}(S_x \boldsymbol{e}_x + S_y \boldsymbol{e}_y) + \frac{g}{T_R}\boldsymbol{e}_z. \tag{4}$$

Here $\boldsymbol{e}_\alpha$, where $\alpha = x, y, z$ denote the unit vectors along the corresponding axes, and the pump pulses are assumed to be weak ($Q \to 1$).

For very weak probe pulses, $q \to 1$, the third term in Eq. (4) vanishes and the average steady state solution gives [45,58]

$$\frac{\langle S_z\rangle}{S_0} = \frac{1}{3}\frac{1 + 3(\Omega_L T_2^*)^2}{1 + (\Omega_L T_2^*)^2}. \tag{5}$$

In zero magnetic field $\Omega_L = 0$, this gives $\langle S_z\rangle/S_0 = 1/3$, as expected for the isotropic hyperfine interaction [23].

For finite probe pulse power $1 - q$, the steady state solution of Eq. (4) can be written as $S_z = g\tau_s^{\rm eff}/T_R$ with the effective spin relaxation time

$$\tau_s^{\rm eff} = \frac{\tau_s T_R \cos^2\theta}{T_R + (1-q^2)\tau_s \sin^2\theta}, \tag{6}$$

where θ is the angle between $\boldsymbol{\Omega}_N + \boldsymbol{\Omega}_L$ and $\boldsymbol{e}_z$. Analytical averaging over the nuclear fields for $\Omega_L = 0$ gives

$$\frac{\langle S_z\rangle}{S_0} = \mu\left[\sqrt{\mu+1}\,\operatorname{arctanh}\left(\sqrt{\frac{1}{\mu+1}}\right) - 1\right], \tag{7}$$

where $\mu = T_R/[\tau_s(1-q^2)]$. Since $T_R \ll \tau_s$, one has $\mu \sim 1$ at $1 - q \ll 1$.

From Eq. (6), one can see that an increase of the probe power (decrease of q) leads to a decrease of the spin relaxation time $\tau_s^{\rm eff}$ and the spin polarization $\langle S_z\rangle$ in agreement with Fig. 1(b). Detailed analysis shows, however, that for the chosen pump power, there are two contributions to the

spin relaxation time: the quantum anti-Zeno effect, described above, and heating of the nuclear spin bath by the probe pulses [59]. Approximately, they contribute to a decrease of $\langle S_z\rangle/S_0$ from 1/3 to 0 and from 1 to 1/3, respectively [28]. The corresponding fit is shown by the orange curve in Fig. 1(b), calculated numerically using the parameters $T_2^* = 0.14$ ns, $\tau_s = 0.5\,\mu$s, and $P_\pi = 103$ mW, and with account for the dynamic nuclear spin polarization. We note the good agreement with the experimental results despite the simplicity of the model as well as the agreement with previous estimates of the system parameters [60,61].

The qualitative explanation of the quantum anti-Zeno effect is sketched at the bottom of Fig. 1. The pump pulse orients the spin polarization along the z axis (i). Due to the strong Overhauser field ($T_2^* \lesssim T_R$), the spin polarization becomes dephased and projected onto the Overhauser field direction ($\mathbf{\Omega}_N$) within the time between the laser pulses (ii). After the dephasing, the action of the probe pulse projects the spin onto the z axis by canceling the transverse spin components (iii). The cancellation varies depending on the probe power, accelerating the spin relaxation and reducing the relative average spin polarization for higher powers at zero magnetic field.

We highlight that the spin relaxation's acceleration is unrelated to a sample heating effect. A higher temperature only changes the electron spin relaxation time τ_s, which is unrelated to the nuclei, and scales the whole PRC without changing its normalized amplitude. Thus, its suppression unequivocally reveals the quantum anti-Zeno effect for the nuclei-induced spin relaxation.

Next, we turn to the quantum Zeno effect, obtained for a long spin dephasing time, $T_2^* \gg T_R$. In this limit, from Eq. (1) for $\Omega_L = 0$, one can see that between the pulses, the in-plane spin components $S_{x/y}$ are increased by $\pm\Omega_{N,y/x}T_R S_z$. On the other hand, according to Eq. (2), the probe and pump pulses reduce them by $(1-q^2Q)S^-_{x/y}$. Thus, in the steady state, $S^+_{x/y} = \pm\Omega_{N,y/x}T_R S_z q^2 Q/(1-q^2Q)$. At the same time, from Eq. (1) we find that the z component of spin decreases between the pulses by

$$S_z^+ - S_z^- = \left[\frac{S_z^+}{\tau_s} + \frac{\left(\Omega_{N,x}^2 + \Omega_{N,y}^2\right)T_R S_z^+}{2} + \Omega_{N,y}S_x^+ - \Omega_{N,x}S_y^+\right]T_R, \tag{8}$$

which is much smaller than S_0. This means that the spin dynamics can be described by the effective spin relaxation time $\tau_s^{\rm eff}$, which is given by

$$\frac{1}{\tau_s^{\rm eff}} = \frac{1}{\tau_s} + \frac{\left(\Omega_{N,x}^2 + \Omega_{N,y}^2\right)T_R(1+q^2Q)}{2(1-q^2Q)}. \tag{9}$$

The steady-state spin polarization similarly to Eq. (3) is given by $S_z^- = g\tau_s^{\rm eff}/T_R$. The averaging over the random nuclear fields can be performed analytically with the result

$$\frac{\langle S_z\rangle}{S_0} = -\nu\,{\rm Ei}(-\nu)\exp(\nu), \tag{10}$$

where $\nu = 4T_2^{*2}(1-q^2Q)/[\tau_s T_R(1+q^2Q)]$ and ${\rm Ei}(x) = -\int_{-x}^{\infty} {\rm e}^{-t}/t\,dt$ is the exponential integral function. This derivation is valid for moderately strong pulses and short pulse repetition periods when $\Omega_N T_R \ll 1 - q^2Q$.

From Eq. (9), one can see that an increase of the probe power (decrease of q) leads to an increase of the spin relaxation time $\tau_s^{\rm eff}$, which is the quantum Zeno effect. This is shown by the orange curve in Fig. 2(b), calculated numerically with the parameters $T_2^* = 88$ ns, $\tau_s = 0.4\,\mu$s, $P_\pi = 80$ mW, $1 - Q = 0.0021$, and $g_e = -0.57$, and describes the experiment quite well, see Ref. [28] for the τ_s and Ref. [44] for T_2^* measurements.

Qualitatively, the quantum Zeno effect can be explained as follows. The pump pulse orients the spin polarization along the z axis (i). After the initialization, the spin starts to precess around the Overhauser field Ω_N (ii). In this case, the $T_2^* \gg T_R$. For weak probe power, the effect of the probe on the transverse spin components is negligible, and the average spin polarization orients itself in the Overhauser field direction, leading to low spin polarization values. Once the probe power increases, it has a stronger impact on canceling the transverse spin components, as sketched at the bottom of Fig. 2, enforcing spin stabilization along the z axis (iii).

For the same reason, the probe pulses decelerate the electron spin precession in a transverse magnetic field. So we measure the electron spin dynamics in the same sample using the extended pump-probe technique [62] for the different powers of the probe pulses. We indeed observe [28] the decrease of the electron spin precession frequency, which demonstrates the quantum measurement back action (quantum Zeno effect) directly in the time dynamics.

Conclusion. In this study, we have demonstrated experimentally and theoretically that the quantum measurement back action allows one to manipulate the spin relaxation time of localized electrons, which is determined by the hyperfine interaction with the nuclear spin fluctuations. The Zeno time of non-Markovian spin dynamics in the studied systems differs by more than two orders of magnitude. It allowed us to observe and describe the quantum anti-Zeno effect for quantum dots and the quantum Zeno effect for donors using the same laser repetition period. The effect of measurement back action on the nuclei-induced spin relaxation was separated from the heating effect by measuring PRC with a pump-probe. As an outlook, we believe that this method will be successfully applied to other systems with localized electrons like colloidal quantum dots, nanoplatelets, perovskites, and moiré quantum dots. Both quantum Zeno effects will be useful for operating spin-photon interfaces generating many-body entangled photon states for quantum information processing.

Acknowledgments. We acknowledge S. A. Tarasenko, D. R. Yakovlev, and N. E. Kopteva for fruitful discussions. The Deutsche Forschungsgemeinschaft provides financial support in the frame of the International Collaborative Research Center TRR 160 (Project A1). M.B. acknowledges support by the Research Alliance Ruhr. N.V.L. and D.S.S. acknowledge the Foundation for the Advancement of Theoretical Physics and Mathematics "BASIS". A.G. and M.B. acknowledge support by the BMBF project QR.X (Contract No. 16KISQ011). The development of the theoretical model by N.V.L. and D.S.S. was supported by the Russian Science Foundation Grant No. 21-72-10035. We acknowledge the quantum dot sample

supply by D. Reuter and A. D. Wieck. The epilayer sample is provided by the Resource Center "Nanophotonics" of Saint Petersburg State University. We acknowledge financial support by Deutsche Forschungsgemeinschaft and Technische Universität Dortmund/TU Dortmund University within the funding programme Open Access Costs.

[1] V. Frerichs and A. Schenzle, Quantum Zeno effect without collapse of the wave packet, Phys. Rev. A **44**, 1962 (1991).

[2] P. Facchi and S. Pascazio, Quantum Zeno and inverse quantum Zeno effects, in *Progress in Optics*, edited by E. Wolf (Elsevier, Amsterdam, 2001), Vol. 42, pp. 147–217.

[3] Edited by K. Kraus, A. Böhm, J. D. Dollard, and W. H. Wootters, *States, Effects, and Operations: Fundamental Notions of Quantum Theory* (Springer, Berlin, 1983).

[4] V. B. Braginsky and F. Y. Khalili, Quantum nondemolition measurements: The route from toys to tools, Rev. Mod. Phys. **68**, 1 (1996).

[5] S. Haroche and J.-M. Raimond, *Exploring the Quantum: Atoms, Cavities, and Photons* (Oxford University Press, Oxford, 2006), pp. 151–161.

[6] A. A. Clerk, M. H. Devoret, S. M. Girvin, F. Marquardt, and R. J. Schoelkopf, Introduction to quantum noise, measurement, and amplification, Rev. Mod. Phys. **82**, 1155 (2010).

[7] R. Raussendorf, D. E. Browne, and H. J. Briegel, Measurement-based quantum computation on cluster states, Phys. Rev. A **68**, 022312 (2003).

[8] H. J. Briegel, D. E. Browne, W. Dür, R. Raussendorf, and M. V. den Nest, Measurement-based quantum computation, Nat. Phys. **5**, 19 (2009).

[9] S. C. Benjamin, B. W. Lovett, and J. M. Smith, Prospects for measurement-based quantum computing with solid state spins, Laser Photon. Rev. **3**, 556 (2009).

[10] L. A. Khalfin, Contribution to the decay theory of a quasi-stationary state, Zh. Eksp. Teor. Fiz. **33**, 1371 (1958) [Sov. Phys. JETP **6**, 1053 (1958)].

[11] B. Misra and E. C. G. Sudarshan, The Zeno's paradox in quantum theory, J. Math. Phys. **18**, 756 (1977).

[12] P. Facchi and S. Pascazio, Quantum Zeno dynamics: Mathematical and physical aspects, J. Phys. A: Math. Theor. **41**, 493001 (2008).

[13] B. Kaulakys and V. Gontis, Quantum anti-Zeno effect, Phys. Rev. A **56**, 1131 (1997).

[14] P. Facchi, H. Nakazato, and S. Pascazio, From the Quantum Zeno to the Inverse Quantum Zeno Effect, Phys. Rev. Lett. **86**, 2699 (2001).

[15] S. Maniscalco, J. Piilo, and K.-A. Suominen, Zeno and Anti-Zeno Effects for Quantum Brownian Motion, Phys. Rev. Lett. **97**, 130402 (2006).

[16] J. D. Franson, B. C. Jacobs, and T. B. Pittman, Quantum computing using single photons and the Zeno effect, Phys. Rev. A **70**, 062302 (2004).

[17] Y. P. Huang and M. G. Moore, Interaction- and measurement-free quantum Zeno gates for universal computation with single-atom and single-photon qubits, Phys. Rev. A **77**, 062332 (2008).

[18] Edited by M. I. Dyakonov, *Spin Physics in Semiconductors* (Springer International Publishing AG, Berlin, 2017).

[19] R. J. Elliott, Theory of the effect of spin-orbit coupling on magnetic resonance in some semiconductors, Phys. Rev. **96**, 266 (1954).

[20] Y. Yafet, *g*-factors and spin-lattice relaxation of conduction electrons, in *Solid State Physics*, edited by F. Seitz and D. Turnbull (Academic, New-York, 1963), p. 2.

[21] G. L. Bir, A. G. Aronov, and G. E. Pikus, Spin relaxation of electrons due to scattering by holes, Zh. Eksp. Teor. Fiz. **69**, 1382 (1975) [Sov. Phys. JETP **42**, 705 (1975)].

[22] M. Dyakonov and V. Perel', Spin relaxation of conduction electrons in noncentrosymmetric semiconductors, Solid State Phys. **13**, 3023 (1972).

[23] I. A. Merkulov, A. L. Efros, and M. Rosen, Electron spin relaxation by nuclei in semiconductor quantum dots, Phys. Rev. B **65**, 205309 (2002).

[24] A. V. Khaetskii, D. Loss, and L. Glazman, Electron Spin Decoherence in Quantum Dots due to Interaction with Nuclei, Phys. Rev. Lett. **88**, 186802 (2002).

[25] W. A. Coish and D. Loss, Hyperfine interaction in a quantum dot: Non-markovian electron spin dynamics, Phys. Rev. B **70**, 195340 (2004).

[26] W. A. Coish and J. Baugh, Nuclear spins in nanostructures, Phys. Status Solidi B **246**, 2203 (2009).

[27] A. V. Shumilin and D. S. Smirnov, Nuclear Spin Dynamics, Noise, Squeezing, and Entanglement in Box Model, Phys. Rev. Lett. **126**, 216804 (2021).

[28] See Supplemental Material at http://link.aps.org/supplemental/10.1103/PhysRevResearch.5.L032032 for the additional quantum anti-Zeno effect measurements for a complementary QDs sample, spin-inertia measurements for the epilayer sample, and additional theoretical details about finding the steady state solution, numerical averaging over the random nuclear fields and comparison of the analytical and numerical calculations.

[29] S. V. Poltavtsev, I. I. Ryzhov, M. M. Glazov, G. G. Kozlov, V. S. Zapasskii, A. V. Kavokin, P. G. Lagoudakis, D. S. Smirnov, and E. L. Ivchenko, Spin noise spectroscopy of a single quantum well microcavity, Phys. Rev. B **89**, 081304(R) (2014).

[30] P. V. Pyshkin, E. Y. Sherman, D.-W. Luo, J. Q. You, and L.-A. Wu, Spatial compression of a particle state in a parabolic potential by spin measurements, Phys. Rev. B **94**, 134313 (2016).

[31] N. V. Leppenen, L. Lanco, and D. S. Smirnov, Quantum Zeno effect and quantum nondemolition spin measurement in a quantum dot–micropillar cavity in the strong coupling regime, Phys. Rev. B **103**, 045413 (2021).

[32] N. V. Leppenen and D. S. Smirnov, Optical measurement of electron spins in quantum dots: Quantum Zeno effects, Nanoscale **14**, 13284 (2022).

[33] G. Hackenbroich, B. Rosenow, and H. A. Weidenmüller, Quantum Zeno Effect and Parametric Resonance in Mesoscopic Physics, Phys. Rev. Lett. **81**, 5896 (1998).

[34] D. V. Khomitsky, L. V. Gulyaev, and E. Y. Sherman, Spin dynamics in a strongly driven system: Very slow Rabi oscillations, Phys. Rev. B **85**, 125312 (2012).

[35] L. Kang, Y. Zhang, X. Xu, and X. Tang, Quantum measurement of a double quantum dot coupled to two kinds of environment, Phys. Rev. B **96**, 235417 (2017).

[36] N. Ahmadiniaz, M. Geller, J. König, P. Kratzer, A. Lorke, G. Schaller, and R. Schützhold, Quantum Zeno manipulation of quantum dots, Phys. Rev. Res. **4**, L032045 (2022).

[37] M. Yamaguchi, T. Asano, and S. Noda, Photon emission by nanocavity-enhanced quantum anti-Zeno effect in solid-state cavity quantum-electrodynamics, Opt. Express **16**, 18067 (2008).

[38] K. J. Xu, Y. P. Huang, M. G. Moore, and C. Piermarocchi, Two-Qubit Conditional Phase Gate in Laser-Excited Semiconductor Quantum Dots Using the Quantum Zeno Effect, Phys. Rev. Lett. **103**, 037401 (2009).

[39] T. Nutz, P. Androvitsaneas, A. Young, R. Oulton, and D. P. S. McCutcheon, Stabilization of an optical transition energy via nuclear Zeno dynamics in quantum-dot–cavity systems, Phys. Rev. A **99**, 053853 (2019).

[40] D. Klauser, W. A. Coish, and D. Loss, Nuclear spin dynamics and Zeno effect in quantum dots and defect centers, Phys. Rev. B **78**, 205301 (2008).

[41] M. T. Mkadzik, T. D. Ladd, F. E. Hudson, K. M. Itoh, A. M. Jakob, B. C. Johnson, J. C. McCallum, D. N. Jamieson, A. S. Dzurak, A. Laucht, and A. Morello, Controllable freezing of the nuclear spin bath in a single-atom spin qubit, Sci. Adv. **6**, eaba3442 (2020).

[42] T. Maimbourg, D. M. Basko, M. Holzmann, and A. Rosso, Bath-Induced Zeno Localization in Driven Many-Body Quantum Systems, Phys. Rev. Lett. **126**, 120603 (2021).

[43] P. Schering, E. Evers, V. Nedelea, D. S. Smirnov, E. A. Zhukov, D. R. Yakovlev, M. Bayer, G. S. Uhrig, and A. Greilich, Resonant spin amplification in faraday geometry, Phys. Rev. B **103**, L201301 (2021).

[44] C. Rittmann, M. Y. Petrov, A. N. Kamenskii, K. V. Kavokin, A. Y. Kuntsevich, Y. P. Efimov, S. A. Eliseev, M. Bayer, and A. Greilich, Unveiling the electron-nuclear spin dynamics in an *n*-doped InGaAs epilayer by spin noise spectroscopy, Phys. Rev. B **106**, 035202 (2022).

[45] M. M. Glazov, *Electron and Nuclear Spin Dynamics in Semiconductor Nanostructures* (Oxford University Press, Oxford, 2018).

[46] A. V. Khaetskii and Y. V. Nazarov, Spin-flip transitions between Zeeman sublevels in semiconductor quantum dots, Phys. Rev. B **64**, 125316 (2001).

[47] L. M. Woods, T. L. Reinecke, and Y. Lyanda-Geller, Spin relaxation in quantum dots, Phys. Rev. B **66**, 161318(R) (2002).

[48] J. Hackmann, D. S. Smirnov, M. M. Glazov, and F. B. Anders, Spin noise in a quantum dot ensemble: From a quantum mechanical to a semi-classical description, Phys. Status Solidi B **251**, 1270 (2014).

[49] D. S. Smirnov, P. Glasenapp, M. Bergen, M. M. Glazov, D. Reuter, A. D. Wieck, M. Bayer, and A. Greilich, Nonequilibrium spin noise in a quantum dot ensemble, Phys. Rev. B **95**, 241408(R) (2017).

[50] I. A. Yugova, M. M. Glazov, E. L. Ivchenko, and A. L. Efros, Pump-probe Faraday rotation and ellipticity in an ensemble of singly charged quantum dots, Phys. Rev. B **80**, 104436 (2009).

[51] E. A. Zhukov, A. Greilich, D. R. Yakovlev, K. V. Kavokin, I. A. Yugova, O. A. Yugov, D. Suter, G. Karczewski, T. Wojtowicz, J. Kossut, V. V. Petrov, Y. K. Dolgikh, A. Pawlis, and M. Bayer, All-optical NMR in semiconductors provided by resonant cooling of nuclear spins interacting with electrons in the resonant spin amplification regime, Phys. Rev. B **90**, 085311 (2014).

[52] P. Schering, G. S. Uhrig, and D. S. Smirnov, Spin inertia and polarization recovery in quantum dots: Role of pumping strength and resonant spin amplification, Phys. Rev. Res. **1**, 033189 (2019).

[53] N. Bohr, The quantum postulate and the recent development of atomic theory, Nature (London) **121**, 580 (1928).

[54] V. B. Braginsky and F. Y. Khalili, *Quantum Measurement* (Cambridge University Press, Cambridge, England, 1992).

[55] E. L. Ivchenko, *Optical Spectroscopy of Semiconductor Nanostructures* (Alpha Science, Harrow UK, 2005).

[56] E. A. Zhukov, D. R. Yakovlev, M. M. Glazov, L. Fokina, G. Karczewski, T. Wojtowicz, J. Kossut, and M. Bayer, Optical control of electron spin coherence in CdTe/(Cd,Mg)Te quantum wells, Phys. Rev. B **81**, 235320 (2010).

[57] Note that the saturation of the optical transition does not affect the ratio $\langle S_z \rangle / S_0$ [28].

[58] D. S. Smirnov, E. A. Zhukov, D. R. Yakovlev, E. Kirstein, M. Bayer, and A. Greilich, Spin polarization recovery and Hanle effect for charge carriers interacting with nuclear spins in semiconductors, Phys. Rev. B **102**, 235413 (2020).

[59] N. Erez, G. Gordon, M. Nest, and G. Kurizki, Thermodynamic control by frequent quantum measurements, Nature (London) **452**, 724 (2008).

[60] E. Evers, N. E. Kopteva, I. A. Yugova, D. R. Yakovlev, D. Reuter, A. D. Wieck, M. Bayer, and A. Greilich, Suppression of nuclear spin fluctuations in an InGaAs quantum dot ensemble by GHz-pulsed optical excitation, npj Quantum Inf. **7**, 60 (2021).

[61] E. A. Zhukov, E. Kirstein, D. S. Smirnov, D. R. Yakovlev, M. M. Glazov, D. Reuter, A. D. Wieck, M. Bayer, and A. Greilich, Spin inertia of resident and photoexcited carriers in singly charged quantum dots, Phys. Rev. B **98**, 121304(R) (2018).

[62] V. V. Belykh, E. Evers, D. R. Yakovlev, F. Fobbe, A. Greilich, and M. Bayer, Extended pump-probe Faraday rotation spectroscopy of the submicrosecond electron spin dynamics in *n*-type GaAs, Phys. Rev. B **94**, 241202(R) (2016).